A F.E.M. MODEL FOR THE EVALUATION OF THE SEISMIC BEHAVIOR OF INTERNAL JOINTS IN REINFORCED CONCRETE FRAMES.

G. Manfredi[1], G.M. Verderame[2] and G.P. Lignola[3]

[1] *Professor, Dept. of Structural Engineering , University of Naples "Federico II", Naples, Italy*
[2] *Assistant Professor, Dept. of Structural Engineering , University of Naples "Federico II", Naples, Italy*
[3] *Assistant Professor, Dept. of Structural Engineering , University of Naples "Federico II", Naples, Italy*
Email: gamanfre@unina.it, verderam@unina.it, glignola@unina.it

ABSTRACT :

The seismic performance of reinforced concrete buildings cannot be fully understood aside from the beam-column joints. The capacity design (and the subsequent strength hierarchy) or the displacement ductility design are modern design principles and they are strongly subordinates to the beam-column joint panels behavior which can reduce substantially the global ductility, if the joint is subjected to a premature failure. Both the cracking of the joint panel zone, the slipping of the passing through steel reinforcement rebars can generate additional deformability and they can alter the strength hierarchy between the elements converging into the beam-column joint. The present work focuses on these two aspects using a refined finite element non-linear modeling technique. A numerical-experimental comparison is discussed that validate the adopted numerical model. Numerical results were compared to experimental data and were found to be in good agreement with the test data, thus validating the methodological approach.

KEYWORDS: Reinforced Concrete, Beam-Column Joint, Shear, Bond, F.E.M. Modelling

1. INTRODUCTION

The behavior of the beam-column joints is a crucial aspect in the seismic design of Reinforced Concrete (RC) structures. The joints are geometrically circumscribed portions of the structures where the high stress transfer from the converging elements burden the concrete core and the reinforcing bars with very high gradients. This aspect can be particularly critical especially in the case of seismic resistant frames where the internal longitudinal steel reinforcement is subjected to tensile loads on one side and compressive loads on the opposite side of the internal joints at opposite column faces. Such conditions are particularly severe for the bond behavior of the passing bars through the joint, especially if it is referred to the high stress states and to the reduced dimensions of the joint core. These aspects, coupled to the mechanical non-linear behavior of the concrete, can cause a reduction of the flexural capacity of the converging elements and a significant variation of their deformability, due to the variation of the stress state in the reinforcing bars at both joint's opposite lateral sections (Hakuto et al., 1999; Fabbrocino et al., 2004).
Usually, according to the main international design codes, the beam-column joint failure is driven by the evaluation of the so-called "Joint Shear" assumed as the main parameter controlling the resultant of all the actions given by the converging elements. The joint shear, V_j, evaluation is based on simple equilibrium equations involving beams and columns (see Figure 1), it is an internal force acting on the free body along the horizontal plane at the midheight of the beam-column connection. In the case of internal joints, the horizontal equilibrium related to the lateral cross sections yields to Eqn. 1.1:

$$V_j = T + C_c' + C_s' - V_c = T' + C_c + C_s - V_c \tag{1.1}$$

Where column shear, V_c, is the shear at the base of the upper column while C_c, C_s and T are, respectively, the force resultant in compression in concrete, and the compressive and tensile resultant in the reinforcing bars. These forces are evaluated on the right side of the joint. On the contrary, the forces evaluated on the left side of the joint are marked with an apex.

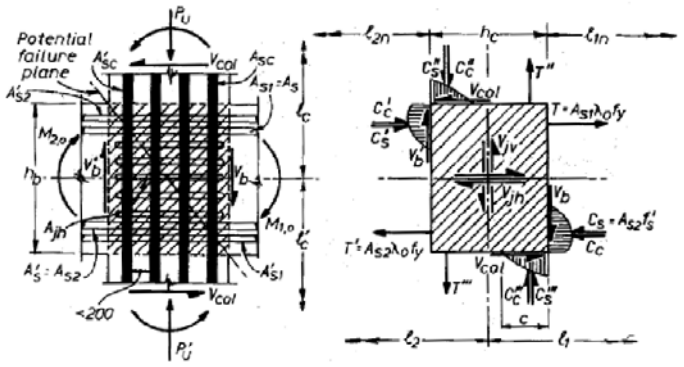

Figure 1. Stress transfer mechanism and free body forces (Paulay and Priestley, 1975).

Accounting also for the cross section internal forces equilibrium, Eqn. 1.1 can be rearranged as:

$$V_j = T' + T - V_C \tag{1.2}$$

The force resultants in tension, *T* and *T'*, can be expressed based on flexural moments in the two lateral sections, *M* e *M'*, and the respective internal moment lever arms, *j* and *j'* assuming that there is no axial force in the beam and assuming a perfect bond between steel bars and surrounding concrete (*pseudo-joint shear*):

$$V_j = \frac{M'}{j'} + \frac{M}{j} - V_C \tag{1.3}$$

the decrease of column shear is attributable to the degradation of flexural strength, due to the reduction of the distance between stress resultants. Thus, the force in compression reinforcement decreases due to the degradation of bond capacity of the beam reinforcements passing through the joint. If the bond capacity of bars is attained, the compressive bars slip causes compressive strain at the opposite column face, where tension should be expected. The reduced compressive force yields to larger height of the compressive zone for concrete thus decreasing the flexural capacity in the beam section at the column face and altering its deformability (see Figure 2).

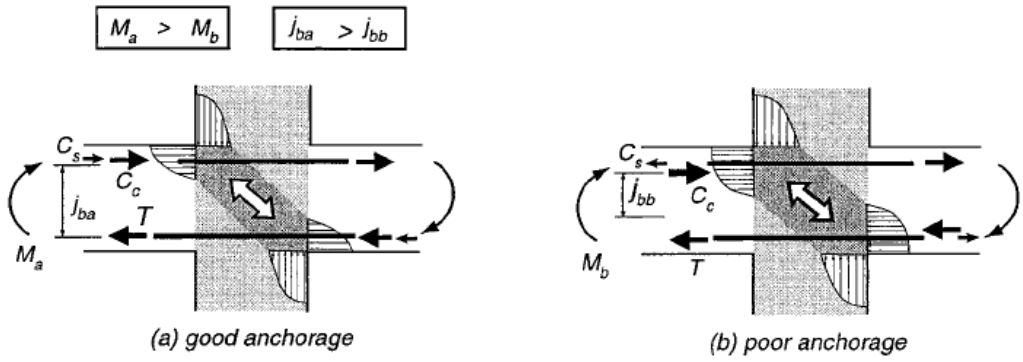

Figure 2. Effect of Anchorage Capacity on moment resistance of beam-column connections (Shiohara, 2001).

The influence of the bond behavior of steel reinforcing bars and surrounding concrete on the global structural behavior of the beam-column joint subassemblage and the joint shear demand is highlighted, referring to a typical interior joint. An interior beam-column joint, tested by Zaid et al. (1999) has been analyzed and modeled by means of a refined Finite Element Method (F.E.M.) analysis. The outcomes of this research campaign confirms the impact of concrete and bond non-linearities on the global and local behavior of tested joint specimen.

2. CASE STUDY: ANALYZED INTERNAL BEAM-COLUMN JOINT

Geometry and test set-up of the analyzed reinforced concrete specimen representing interior beam-column joint subassemblages, named S3, without transverse beams, tested by Zaid et al. (1999) are reported in figure 3a. Boundary conditions are shown: the beam ends were supported by horizontal rollers, while the bottom of the column was supported by a universal pin. The distance between the two hinges for beams and columns were 2,700 mm and 1,470 mm respectively. The top of the column was loaded by two actuators in vertical and horizontal directions. The vertical actuator provided a constant axial load of 100 kN, while the horizontal one provided a statically horizontal cyclic load by displacement control simulating story shear under earthquake actions.

S3 specimen was designed to attain a joint shear failure mode by increasing the amount of beam bars passing through the joint, having though conventional reinforcing detail. Also the dimensions of the members are commonly adopted in internal beam-column joints. The section of the columns and beams were 300x300mm^2 and 300x200mm^2 respectively. Figure 3b shows the geometry and reinforcement arrangement of the specimen.

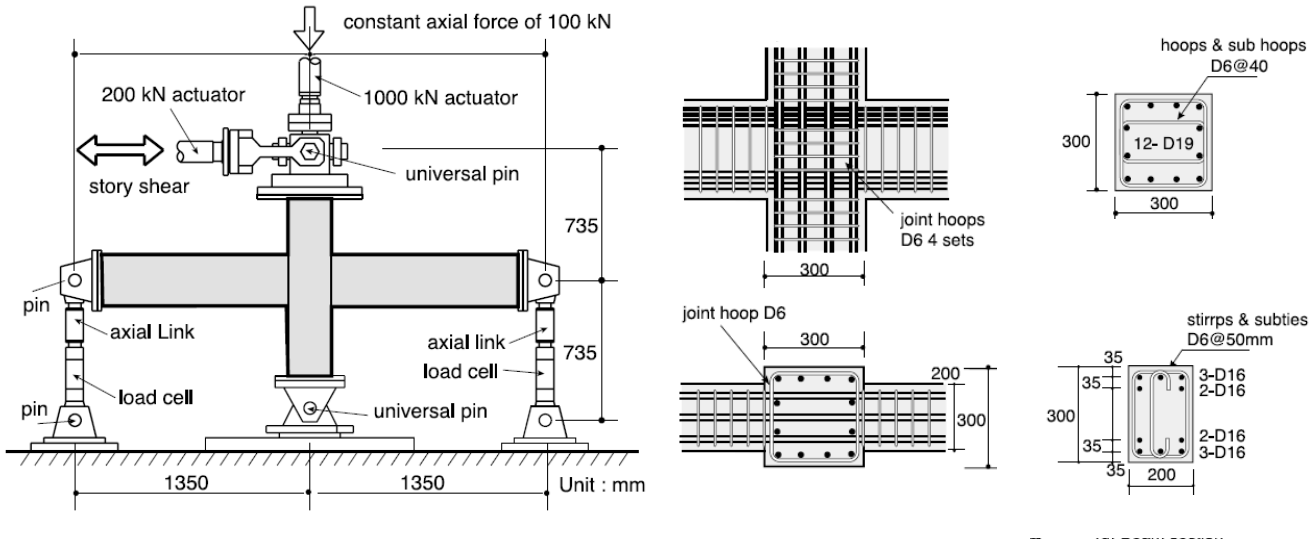

a) b)

Figure 3. Zaid et al. (1999): a) Loading system; b) Geometry of the beam-column connection and reinforcement arrangement.

Five D16 bars were arranged at the top and the bottom of the section of the beams. Reinforcement in columns is also common and 12-D19 bars were used. Four sets of stirrups of D6 bars were supplied with a spacing of 40 mm in the column and 50 mm in the beam.

A normal concrete with mean compressive strength of 28.0 MPa (according to the test of 100x200mm^2 cylinders) was adopted. The SD390 steel was used for D16 and D19 bars while SD345 steel was used for D6 bars. The mechanical properties of the deformed bars are reported in Table 2.1.

Table 2.1. Mechanical properties of steel bars.

Reinforcing bars diameter	Nominal sectional area [mm^2]	Yield Strength [MPa]	Young's Modulus [GPa]
D6	32	390	185
D16	199	470	194
D19	287	450	208

3. F.E.M. ANALYSIS

An accurate numerical analysis has been performed modeling the discussed several critical aspects on joints behavior using the multipurpose finite-element analysis software DIANA v9.1, which can handle accurate bi-dimensional analyses (de Witte and Kikstra 2005). Starting from detailed geometric sketches of the tested specimen S3, the full interior beam-column joint subassemblage was modeled by more than 3,000 eight-nodes, bi-dimensional plane stress elements, based on non-linear material properties. To have a more refined structured mesh close to the joint core, the elements size was biased with a grading factor and decreasing size toward the joint core panel. In figure 4a is reported the mesh adopted for the concrete material.

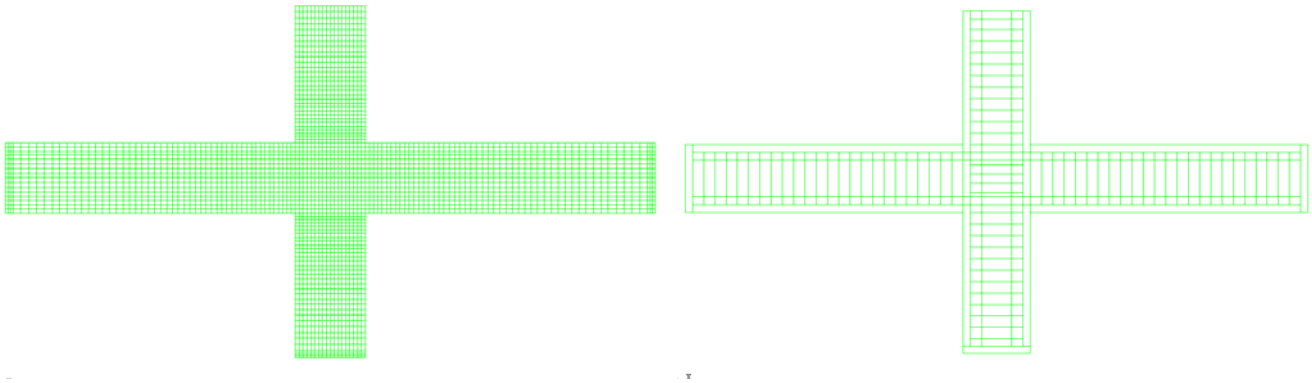

a) b)

Figure 4. Adopted mesh: a) concrete material; b) steel longitudinal and transverse reinforcement.

Mechanical properties of involved materials simulate the non-linear behavior in compression (plasticity) and tension (cracking for concrete and yielding for steel). The Mander et al. (1988) model was adopted for concrete in compression, and the parameters adopted take into account in detail the confinement due to the transverse steel reinforcement: confined concrete strength and corresponding strain are f_{cc}=36 MPa and ε_{cc}=0.48%, respectively. Conversely, unconfined concrete strength and corresponding strain are f_{co}=28 MPa and ε_{co}=0.20%. In both cases the concrete cracking behavior is simulated with a linear elastic branch up to tensile strength of 2.67 MPa followed by an exponential tension softening branch.

An ideal plasticity model without hardening was adopted for steel reinforcement both in tension and compression considering for each reinforcing bar diameter (see table 2.1) the effective yield strength and Young's Modulus. Transverse reinforcement was modeled assuming perfect bond between the bars and the surrounding concrete and 967 two-nodes special reinforcement elements were adopted. Conversely the longitudinal reinforcement was not perfectly bonded to the embedding elements. For non-linear analysis on beam-column joints, the embedded formulation with perfect bond is too coarse. For such case, separate 759 three-nodes truss elements for the reinforcement were adopted and connected to the surrounding structural concrete via structural interface elements. These 3+3-nodes interface elements facilitate bond-slip analysis based on non-linear Model Code 90 (CEB-FIP Model Code, 1990) τ - *slip* relationship, depicted in figure 5a where the bond strength is,

$$\tau_{\max} = 1.25\sqrt{f_{ck}} \qquad (3.1)$$

In the present work it is assumed f_{ck} equal to f_{co}. This formulation is valid for ribbed reinforcing steel in confined concrete in not good bond condition (according to code definitions). In figure 5b the bond stress-slip function under monotonic loading is reported where characteristic slip values s_1 and s_2 are equal to 1 mm and 3 mm, respectively, while s_3 is the clear rib spacing (9 mm). Furthermore the coefficient α is taken equal to 0.4 and the residual bond capacity, τ_f, is 0.40 τ_{max}.

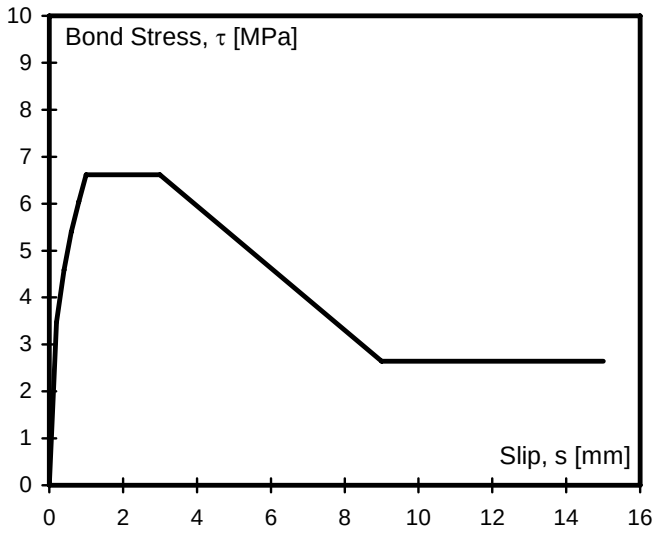

a)

$$\tau = \tau_{\max}\left(\frac{s}{s_1}\right)^{\alpha} \qquad 0 \le s \le s_1$$

$$\tau = \tau_{\max} \qquad s_1 \le s \le s_2$$

$$\tau = \tau_{\max} - \left(\tau_{\max} - \tau_f\right)\frac{s - s_2}{s_3 - s_2} \qquad s_2 \le s \le s_3$$

$$\tau = \tau_f \qquad s \ge s_3$$

b)

Figure 5. Bond stress-slip relationship under monotonic loading: a) diagram plot, b) analytical functions

3.1. Experimental-Numerical Comparisons

Figure 6a compares column shear-story drift relation for specimen S3. Tested specimens S3 experienced a degradation of story shear and clear pinching loops due to joint shear deformation and due to decay of shear force after story drift 2% when the attained maximum story shear was 128.4 kN. The numerical analysis predicts accurately the ascending portion of the diagram both in terms of shear force and stiffness, while the post peak softening, probably due to the cyclic decay in tested specimen and not simulated in monotonic F.E.M. analysis, was missed. Envelope curves of the joint shear are plotted against story drift in figure 6b. It is observed that relation between joint shear and story drift for the tested specimen S3 is very similar to that of the numerical model, even if it was not true in column shear-story drift relation after story drift 2%. Joint shear stress results continuously increasing as story drift increases.

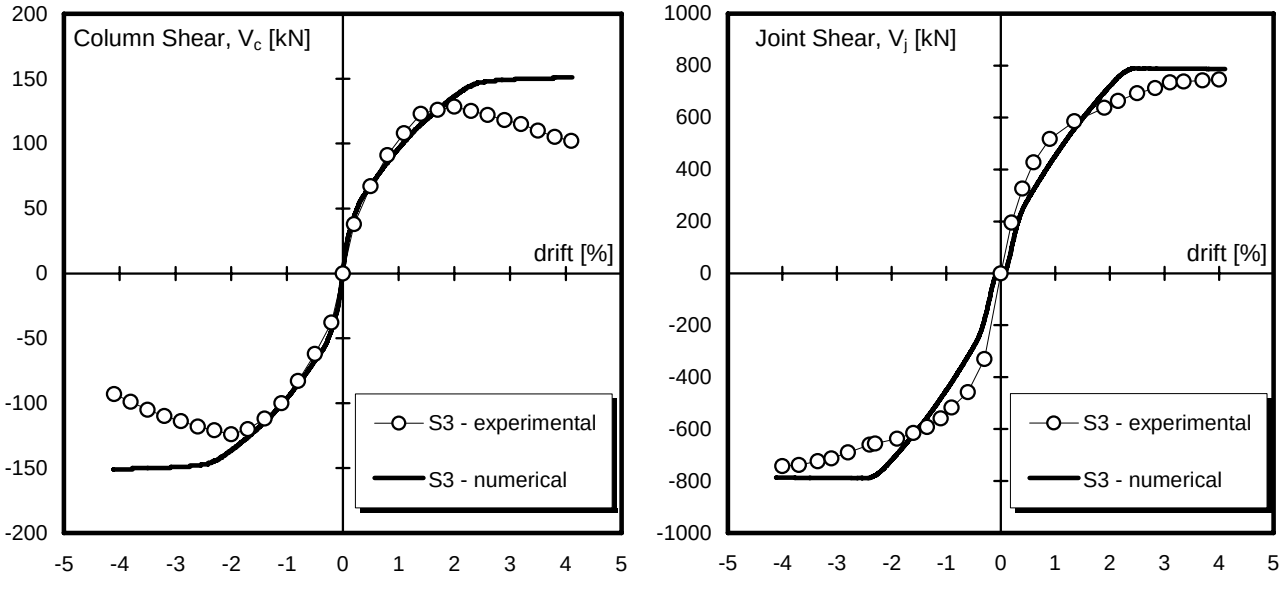

a) b)

Figure 6. Experimental-Numerical Comparisons: a) column shear, b) joint shear

It is highlighted that, according to the joint shear definition in Eqn 1.2, the column shear is negligible if compared to the yielding force in the longitudinal beam reinforcement. Hence, it is concluded that the increase of joint shear deformation and the degradation of the column shear observed in specimen S3 was not caused by the degradation of the joint shear stress. According to these results, it seems that joint shear is an inappropriate index for evaluation of the vulnerability of beam-column joints to joint shear failure, in fact the joint shear stress increases even after apparent beginning of joint shear failure as well as after deterioration of story shear.
Figure 7a shows the relation of anchorage force in beam bars and story drift angle. The anchorage force can be defined as the difference of total forces, T' and T, in longitudinal beam bars at two opposite column faces. This force is due to the bond between steel bars and surrounding concrete. The force in beam bars was evaluated on steel plastic perfectly plastic stress-strain relationship referring to strain data along the upper central longitudinal bars through joint core read by strain gauges during test and on the numerical model in F.E.M. analysis.
Figure 7b compares upper longitudinal bars stress-story drift relation at two opposite column faces of specimens S3. The numerical analysis predicts quite well the diagrams related to both sides. When the story drift exceeds 3%, yielding of tensile reinforcement in tested specimen beams occurred at the column face. At story drift of 2%, the modeled beam bars showed yielding. It is noted that tensile stress is assumed positive. In figure 7b it is clearly noted that the stress in tensile reinforcement is in tension up to the yielding strain, while, when the anchorage resistance attained its capacity, the stress in compressive reinforcement at the right column face shifted from compression to tension.

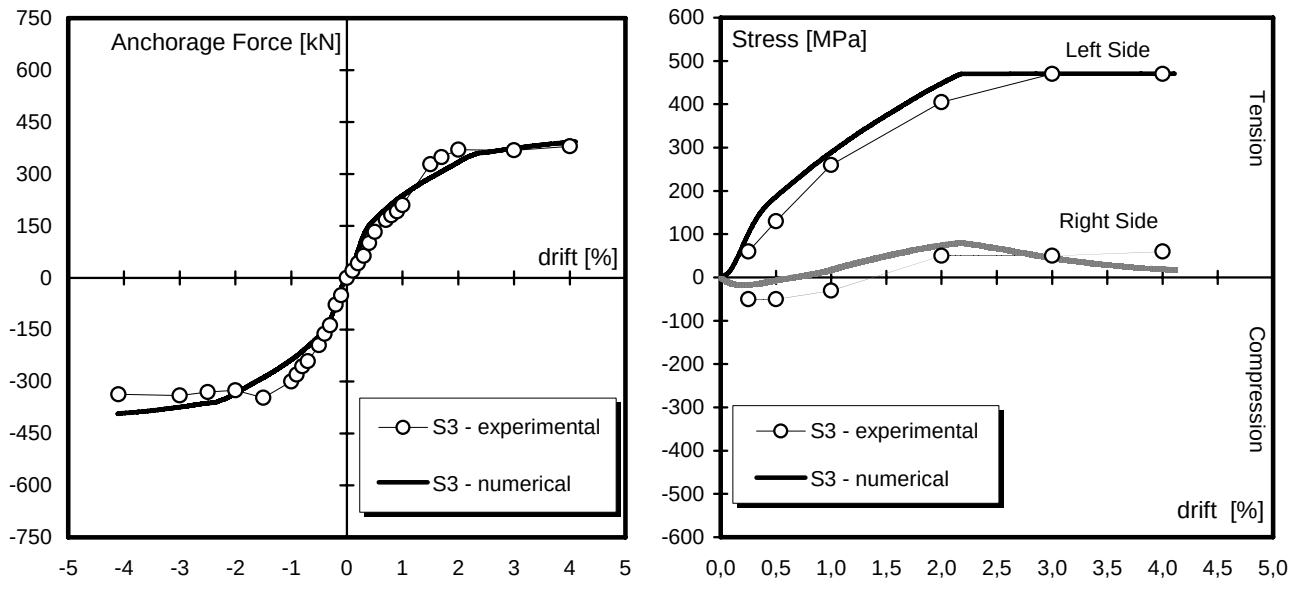

a) b)

Figure 7. Experimental-Numerical Comparisons: a) anchorage force, b) reinforcement stress

The bond slip changes force in compressive bars to tension, thereby the compressive force carried by concrete is increased. As a consequence the location of compressive stress resultants shift to center of beam leading to reduction of the internal moment lever arm as shown in figure 2. Furthermore this leads to deterioration of flexural strength and especially of deformability of the beams and thereby the reduction of the story shear cannot be related to the, almost always, increasing shear force.
The numerical analysis is able to simulate this complex phenomena. Moreover very good agreement is found between experimental outcomes and numerical simulations. In fact the tested specimen S3 was designed such that joint failure would initiate before beam's flexural yielding by using large amount of beam bars passing through the joint (Zaid et al. 1999). It is noted that the joint shear failure occurred at story drift 2% and then the flexural yielding of beams occurred at story drift 3% in the specimen S3.
The cracking patterns of tested specimen S3 and numerical model at story drift 3% are shown in figure 8. It is

recalled that the experimental test contemplate cyclic loading with paired cycles of the same amplitude in story drift repeated to simulate actual earthquake load, while the numerical analysis was conducted under monotonic loads. Flexural cracks in beams were uniformly distributed over the whole length of beams on both the top and the bottom of the beams in the tested specimen, while they are plotted only on tensile side (top on the left and bottom on the right) of the beams in the numerical model.

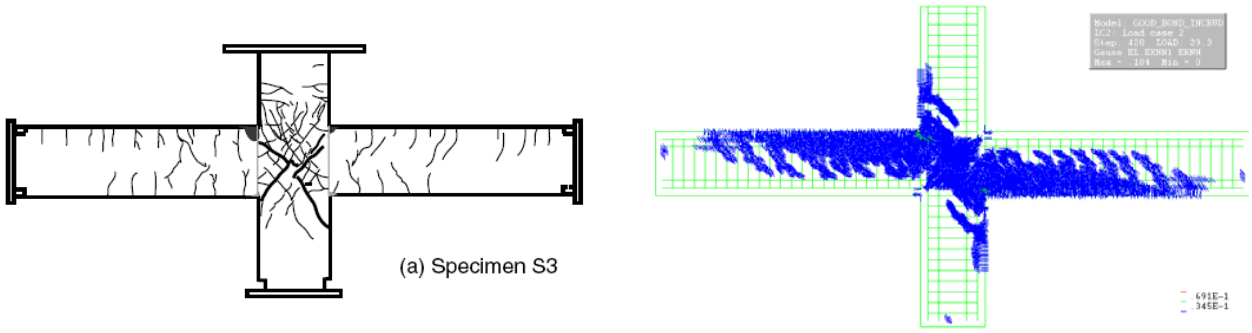

a) b)

Figure 8. Observed crack pattern at story drift 3.0%: a) during cyclic test (Zaid et al., 1999), b) numerical monotonic outcome.

It is clearly seen the diagonal compressive concrete strut in the joint core in figure 9 which is parallel to the cracking planes, furthermore the flexural failure is visible in the beam section at the opposite column faces (vertical cracks on tension side and concrete crushing on compression side). The higher is the bond strength, the lower is the crack width in concrete because of the improved stress transfer provided by the ribbed bars.

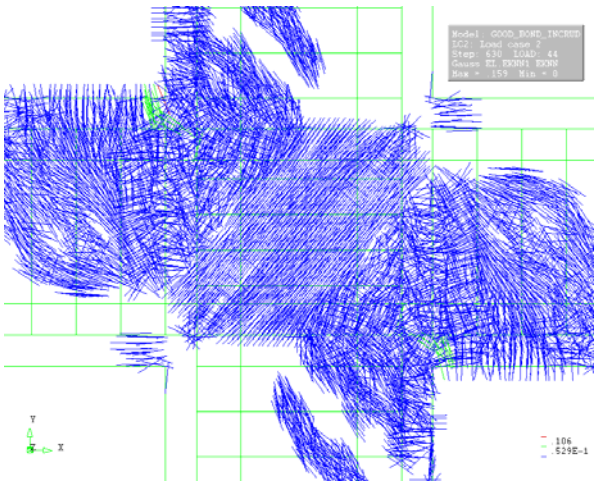

Figure 9. Numerical F.E.M. crack pattern. Detail of the beam column joint core panel at story drift 3.0%.

4. CONCLUSIONS

Stress transfer mechanisms between beams and columns converging in the joint core panel depend on several aspects, sometimes able to invalidate the capacity design (and the subsequent strength hierarchy). Outcomes of the reported test campaign on twenty specimens failed in joint shear failure mode highlighted that the fundamental cause of deterioration in story shear can be identified as the reduction in anchorage capacity of beam reinforcing bars through the joint core so that the impact of concrete and bond non-linearities on the

global and local behavior of joints is crucial.
Furthermore the so-called "joint Shear" is an inappropriate index for the evaluation of vulnerability of beam-column joints to joint shear failure, even though it is usually assumed as the main parameter controlling this failure mode. In fact the joint shear stress increases even after apparent beginning of joint shear failure as well as after deterioration of story shear. The joint shear force and story shear force are not proportional.
The cause of the degradation in story shear is due to the anchorage capacity of beam longitudinal reinforcement passing through the beam-column joint panel. When the anchorage stress attains its capacity, stress in compressive reinforcement at the column face shifts from compression to tension. The loss of compressive load carrying capacity of the compressive reinforcement in the section at the column face causes an increase in the compressive force carried by concrete. This leads to a shift of compressive resultants to the center of beam leading to a reduction of the internal moment lever arms followed by a deterioration of flexural strength and especially of deformability of the beams. All these phenomena acting together lead to a global reduction of the beam-column joint performances. FEM analyses have been adopted as a tool to simulate in great detail all these crucial aspects. Numerical results were compared to experimental outcomes and they were found to be in good agreement with the test data, thus validating the methodological approach.

5. ACKNOWLEDGMENT

The analyses were developed within the activities of Rete dei Laboratori Universitari di Ingegneria Sismica – ReLUIS for the research program funded by the Dipartimento di Protezione Civile – Progetto Esecutivo 2005-2008.

REFERENCES

CEB-FIP Model Code (1990), "Design Code". Comité Euro-Intermational du Béton, Lausanne, Switzerland, Thomas Telford.
de Witte F.C., Kikstra W.P. (2005). "DIANA Finite Element Analysis. User's Manual. Analysis Procedures". Delft, The Netherlands. TNO DIANA bv.
Fabbrocino G., Verderame G.M, Manfredi G., Cosenza E. (2004). "Structural models of critical regions in old type r.c. frames with smooth rebars". *Engineering Structures*, **26:14**, 2137-2148.
Hakuto, S., Park, R., Tanaka, H. (1999). "Effect of deterioration of bond of beam bars passing through interior beam-column joints on flexural strength and ductility". *ACI Structural Journal*, **96:5**,858-864.
Mander, J.B., Priestley, M.J.N., Park, R., (1988). "Theoretical stress–strain model for confined concrete". *Journal of the Structural Division ASCE* **114**,1804–1826.
Paulay, T., Priestley, M.J.N. (1975). "Seismic Design of Reinforced concrete and masonry buildings" Wiley, New York
Shiohara H. (2001). "New Model for Shear Failure of RC Interior Beam-Column Connections". *ASCE J. Struct. Engrg.*, **127:2**,152-160
Zaid, S., Shiohara, H., Otani, S. (1999). "Test of a joint reinforcing detail improving joint capacity of r/c interior beam-column joint". The 1st Japan-Korea Joint Seminar on Earthquake Engineering for Building Structures, Seoul National University, Seoul, Korea